

Role of Electric Field in the Formation of Detached Regime in Tokamak Plasma

I.Senichenkov¹, E. Kaveeva¹, V. Rozhansky¹, E. Sytova¹⁻⁴, I. Veselova¹, S. Voskoboynikov¹,
D. Coster²

¹*Peter the Great St.Petersburg Polytechnic University, Saint Petersburg, Russia*

²*Max-Planck Institut für Plasmaphysik, EURATOM Association, D-85748, Garching, Germany*

³*Ghent University, Ghent, Belgium*

⁴*Aix-Marseille Université, Marseille, France*

E-mail: I.Senichenkov@spbstu.ru

Received at 17th October 2017

Abstract A modeling of the transition to the detachment of ASDEX Upgrade tokamak plasma with increasing density is performed by the SOLPS-ITER numerical code with a self-consistent account of drifts and currents. Their role in plasma redistribution both in the confinement region and in the Scrape-off Layer (SOL) is investigated. The mechanism of the High Field Side High Density formation in the SOL during the transition to the detachment is suggested. In the full detachment regime, when the cold plasma region expands above the X-point and reaches closed magnetic flux surfaces, the plasma perturbation in the confined region might lead to the change in the confinement regime.

DOI: 10.21883/0000000000

According to the current understanding of divertor physics, at least partial detachment will be a necessary condition for operation of future fusion power devices [1,2]. In this regime 80% of thermonuclear power coming in the form of convective and conductive fluxes is irradiated near the divertor targets. This allows for target shielding from heat fluxes and for meeting the material heat loads requirements. In experiments it is demonstrated that a successful transition to the detachment may be achieved either with increasing the plasma density (e.g. by the increasing of a gas puff) or by radiative impurity seeding (nitrogen, neon, argon). However, physical mechanisms of the transition are still not well understood. Consequently, the detached regime is now actively studied theoretically and experimentally (see, e.g. [3-7]) focusing on the impurity transport [8]. And if the qualitative picture of the transition is more or less clear (see e.g. [9]), attempts to perform corresponding calculations which would coincide to experiment are still not successful.

In the present paper the transition to detached divertors with increasing density of the plasma of ASDEX Upgrade tokamak with carbon divertor plates (before the installation of a full

tungsten wall) is modelled by the numerical code SOLPS-ITER [10]. This code solves the fluid transport equations [11] with self-consistent account of electric field, ExB drift, diamagnetic drift and currents. The aim of the work is to investigate their role in fluxes redistribution and in the transition to detachment.

As a base modeling scenario the ASDEX Upgrade shot #17151 (with carbon impurity) [12] is chosen. This is a standard regularly reproducible discharge former used for testing and benchmarking of the earlier versions of the SOLPS-ITER code. In the quasi-stationary phase of this discharge the deuterium income due to the Neutral Beam Injection (NBI) was compensated by pumping (gas puff was turned off). In the carbon particle balance the pumping rate was equal to the income due to the target sputtering. The discharge power $P \approx 3$ MW in the modeling is provided by prescription of temperature values at the core boundary, and the anomalous transport coefficients are chosen so that the density and temperature profiles fit experimental ones in the equatorial midplane and at targets.

Transition to the detachment is modelled by the increasing the density n_e at the core boundary and a corresponding decrease of the electron and ion temperatures, T_e and T_i , keeping the product $n_e(T_e + T_i)$ constant. Thus the anomalous heat conductivity fluxes $n_e(\chi_{e\perp}^{(AN)}\nabla_{\perp}T_e + \chi_{i\perp}^{(AN)}\nabla_{\perp}T_i)$ and conductive heat flux caused by anomalous diffusion $\frac{5}{2}T_e D_{\perp}^{(AN)}\nabla_{\perp}n_e$ – which give main contribution to the discharge power crossing the separatrix – remain almost constant too. Here $\chi_{e\perp}^{(AN)}$, $\chi_{i\perp}^{(AN)}$, $D_{\perp}^{(AN)}$ are the perpendicular (with regards to the B-field) anomalous transport coefficients. All the rest modeling parameters remain unchanged. Three modeling scenarios are considered with flux surface averaged main ion (deuterium) density at the core boundary: $\langle n_i \rangle = 4.0 \cdot 10^{19} \text{ m}^{-3}$ (base one), $\langle n_i \rangle = 8.0 \cdot 10^{19} \text{ m}^{-3}$ and $\langle n_i \rangle = 12.0 \cdot 10^{19} \text{ m}^{-3}$. Here $\langle \dots \rangle$ denotes the flux surface averaging, and the difference between n_e and n_i due to the presence of impurities is assumed to be negligible. Strictly speaking, these modeling scenarios do not correspond to the real experimental scenario, where the density increase was reached by gas puff, however, the chosen density values are typical for the experiment.

In the base scenario ($\langle n_i \rangle = 4.0 \cdot 10^{19} \text{ m}^{-3}$) the inner divertor is detached and outer is in high recycling regime. For $\langle n_i \rangle = 8.0 \cdot 10^{19} \text{ m}^{-3}$ and $\langle n_i \rangle = 12.0 \cdot 10^{19} \text{ m}^{-3}$ the outer divertor also becomes detached. This may be seen by the most evident sign of the transition – the decrease of the electron temperature (Fig. 1). Near the detached target it falls down to the level of about 1 eV, so that the volume recombination starts to exceed the recombination on the target. The

particle fluxes to the targets decrease correspondingly in spite of the increase of the electron density – this is the so-called roll-over effect, and it is also reproduced in the modeling.

Calculations demonstrate that the strong electric field may appear near the detached divertors, and the corresponding electric potential overcomes T_e/e . To see how such a field appears let's analyze the parallel (with respect to the B-field) projection of the electron force balance equation

$$j_{\parallel}/\sigma_{\parallel} = E_{\parallel} + \nabla_{\parallel}(n_e T_e)/en_e + 0.71\nabla_{\parallel}T_e/e \quad (1)$$

where E_{\parallel} is a parallel electric field and σ_{\parallel} is a Spitzer conductivity.

The parallel current j_{\parallel} consists of the thermoelectric current caused by plasma temperature difference near outer and inner targets and of Pfirsch-Schlüter current, which closes the divergent part of perpendicular currents, mainly the diamagnetic one. Here it is assumed that the Pfirsch-Schlüter current can be partially closed through divertor targets, not only inside the plasma.

Let's consider the hot outer target and cold (detached) inner one. Near the outer target, where the electron temperature T_e is high, the Spitzer conductivity is high too, so that the whole expression in the r.h.s. of (1) is small compared to any of three terms it consists of. In other words, electric force almost compensates the **pressure gradient** and thermal forces, and the electric potential remains of the order of T_e/e . In the cold plasma near the inner target, where $T_e \approx 1$ eV and Spitzer conductivity is significantly smaller, the electron parallel force balance reduces to the Ohm's law in its simplest form

$$j_{\parallel}/\sigma_{\parallel} \approx E_{\parallel} \quad (2)$$

Indeed, in the cold plasma the l.h.s. of (1) is no more small, since the conductivity reduces, while the current density does not, since the main contribution to it is the thermoelectric current flowing from the hot target. Since the temperature near inner target is small, the **pressure gradient** and the thermal force in the r.h.s. of (1) are also small, and the big current is provided by the electric field. In the Fig. 2 shown is the transition from the full force balance (1) to the simplified Ohm's law (2) with the motion from the hot plasma above the X-point towards the cold plasma near the inner target.

Strong electric field appears also in the Private Region (PR) below the X-point, where similarly it is necessary to drive the current through the cold plasma towards targets. However, in this region the main contribution to the current density is given by the Pfirsch-Schlüter current, which closes the ∇B - drift induced current penetrating here from the confined region and from the outer part of the scrape-off layer.

Detailed analysis of computational results shows that there exists an electric potential maximum, which corresponds to the strong electric field. This maximum is located at the boundary between cold and hot plasma both in the SOL and in PR, to provide strong electric field in the cold plasma (see Fig. 3)

The ExB-drift velocity of charged particles is directed along the equipotential surfaces round the electric potential maximum. When this maximum appears in the X-point vicinity, drift fluxes drug particles from the SOL near the outer target through the PR towards the SOL near the inner target. This leads to the density increase in the SOL there, and similar density rise is observed in experiments and is known as High Field Side High Density (HFSHD).

During the transition to the more pronounced detachment regime (in our modeling – with increasing discharge density) the area occupied by cold plasma increases in size, and the boundary mentioned above together with the locus of electric potential maximum move towards the X-point (Figs. 1-3). In the full detachment the cold area becomes so large that neutral atoms can penetrate through the separatrix into the confined zone causing its cooling. This effect is seen in the modeling results and is observed in the experiment also.

At the same time as the plasma near the outer target transits to the detached regime, the temperature near targets equilibrates, the thermoelectric current reduces, causing the reduction of the total longitudinal current and the electric field in the SOL. Due to this E-field reduction the HFSHD disappears in the full detachment. Reduction of the parallel current causes the reduction of the total current flowing to the target; such a reduction is seen in the experiment, and sometimes is considered as a sign of the transition to the detachment [5].

It is worth mentioning that the reduction of E-field in the SOL does not necessarily causes the reduction of E-field in the PR. i.e. the potential maximum may still remain below the X-point.

The vortex flow round the potential maximum, which is located near the X-point, affects the plasma on closed flux surfaces and may contribute to the net particle flux through the separatrix.

In general, the presence of a spot of cold plasma above the X-point, where the temperature is about several eVs, changes the transport in the confined region significantly. The big ionization sources rises in this cold spot, and ions born here either flow along the magnetic field lines or are drugged outside the separatrix by diffusion and ExB-drift. Structure of parallel flows changes significantly in comparison to unperturbed surfaces, viscous flows and current changes correspondingly. These changes might lead to the change of the radial electric field shear, poloidal rotation shear and the level of turbulence. Thus the transition to the detachment may affect the global plasma confinement.

Work is done in the Peter the Great Saint Petersburg Polytechnic University under support of the Russian Scientific Foundation, Grant No. 17-12-01020. Numerical calculations are performed in the SuperComputer Center “Polytechnic” in the Peter the Great SPbPU.

Литература

- [1] R.A.Pitts, S.Carpentier, F.Escourbiac, T.Hirai, V.Komarov, A.S.Kukushkin, S.Lisgo, A.Loarte, M.Merola, R.Mitteau, A.R.Raffray, M.Shimada, P.C.Stangeby. // *Journal of Nuclear Materials* **415** (2011) S957–S964
- [2] A.R.Raffray, R.Nygren, D.G.Whyte, S.Abdel-Khalik, R.Doerener, F.Escourbiac, T.Evans, R.J.Goldston, D.T.Hoelzer, S.Konishi, P.Lorenzetto, M.Merola, R.Neu, P.Norajitra, R.A.Pitts, M.Rieth, M.Roedig, T.Rognien, S.Suzuki, M.S.Tillack, C.Wong. // *2010 Fusion Eng. Des.* **85** 93–108
- [3] S. Potzel, M. Wischmeier, M. Bernert, R. Dux, H.W. Müller, A. Scarabosio and the ASDEX Upgrade Team. // *Nucl. Fusion* **54** (2014) 013001
- [4] F. Reimold, M. Wischmeier, M. Bernert, S. Potzel, A. Kallenbach, H.W. Müller, B. Sieglin, U. Stroth and the ASDEX Upgrade Team. // *Nucl. Fusion* **55** (2015) 033004
- [5] A. Kallenbach, M. Bernert, M. Beurskens, L. Casali, M. Dunne, T. Eich, L. Giannone, A. Herrmann, M. Maraschek, S. Potzel, F. Reimold, V. Rohde, J. Schweinzer, E. Viezzer, M. Wischmeier and the ASDEX Upgrade Team. // *Nucl. Fusion* **55** (2015) 053026
- [6] F. Reimold, M. Wischmeier, S. Potzel, L. Guimaraes, D. Reiter, M. Bernert, M. Dunne, T. Lunt, the ASDEX Upgrade team, the EUROfusion MST1 team. // *The high field side high density region in SOLPS-modeling of nitrogen-seeded H-modes in ASDEX Upgrade*, *Nuclear Materials and Energy* (2017), <http://dx.doi.org/10.1016/j.nme.2017.01.010>
- [7] A R Field, I Balboa, P Drewelow, J Flanagan, C Guillemaut, J R Harrison, A Huber, V Huber, B Lipschultz, G Matthews, A Meigs, J Schmitz, M Stamp, N Walkden and JET contributors. // *2017 Plasma Phys. Control. Fusion* **59** 095003
- [8] Кавеева Е.Г., Бекхейт А.Х., Воскобойников С.П., Рожанский В.А., Костер Д., Боннин К., Шнейдер Р. // *Письма в ЖТФ*. Том **29**. Вып. 5, стр. 87 (2003)
- [9] S.I. Kraseninnikov, A.S. Kukushkin and A.A. Pshenov. // *Physics of Plasmas* **23**, 055602 (2016); doi: 10.1063/1.4948273
- [10] X. Bonnin, W. Dekeyser, R. Pitts, D. Coster, S. Voskoboynikov and S. Wiesen. // *Plasma and Fusion Research* **11** (2016) 1403102
- [11] V. Rozhansky, E. Kaveeva, P. Molchanov, I. Veselova, S. Voskoboynikov, D. Coster, G. Counsell, A. Kirk, S. Lisgo, the ASDEX-Upgrade Team and the MAST Team. // *Nuclear Fus.* **49** 025007 (2009)
- [12] A.V. Chankin, D.P. Coster, R. Dux, Ch Fuchs, G Haas, A Herrmann, L D Horton, A Kallenbach, M Kaufmann, Ch Konz, K Lackner, C Maggi, H W Müller, J Neuhauser, R Pugno, M Reich and W Schneider. // *Plasma Phys. Control.Fusion.* **48** 839 (2006)

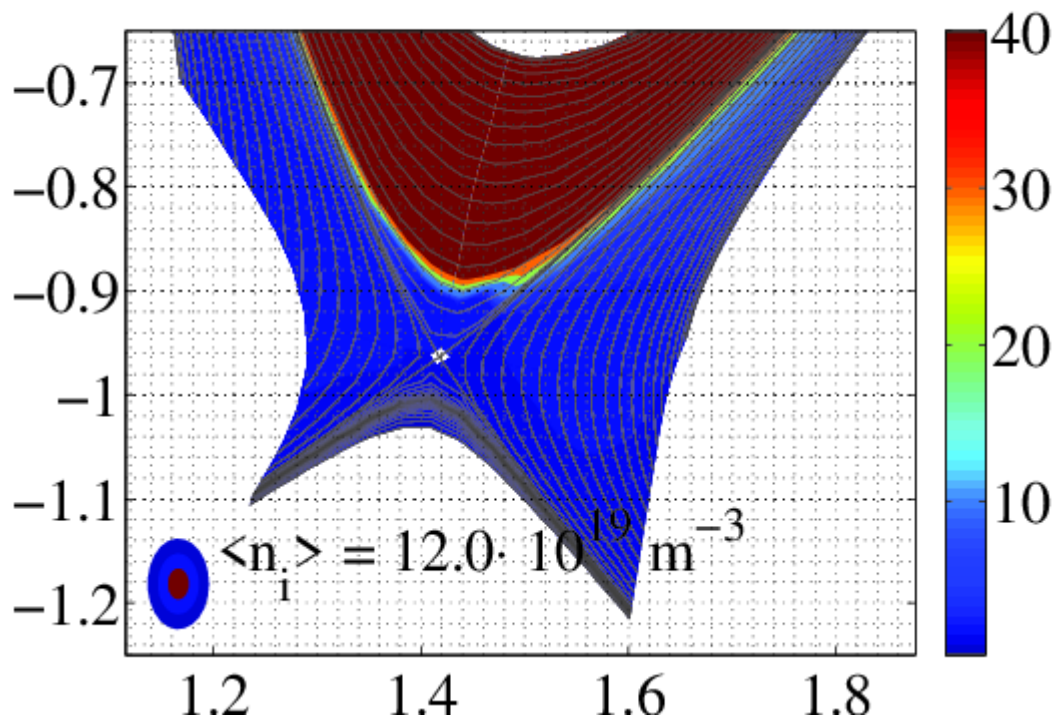
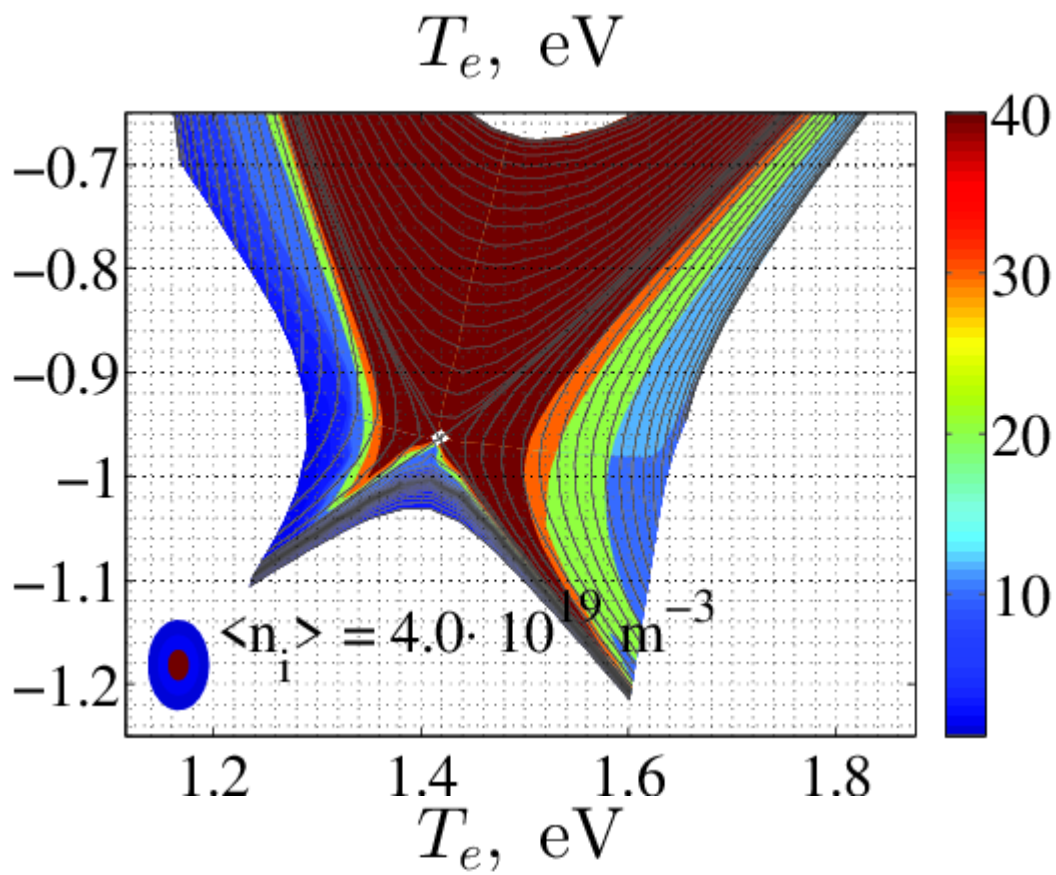


Figure 1. Calculated electron temperature for different plasma density a) $\langle n_i \rangle = 4.0 \cdot 10^{19} \text{ m}^{-3}$ and b) $\langle n_i \rangle = 12.0 \cdot 10^{19} \text{ m}^{-3}$.

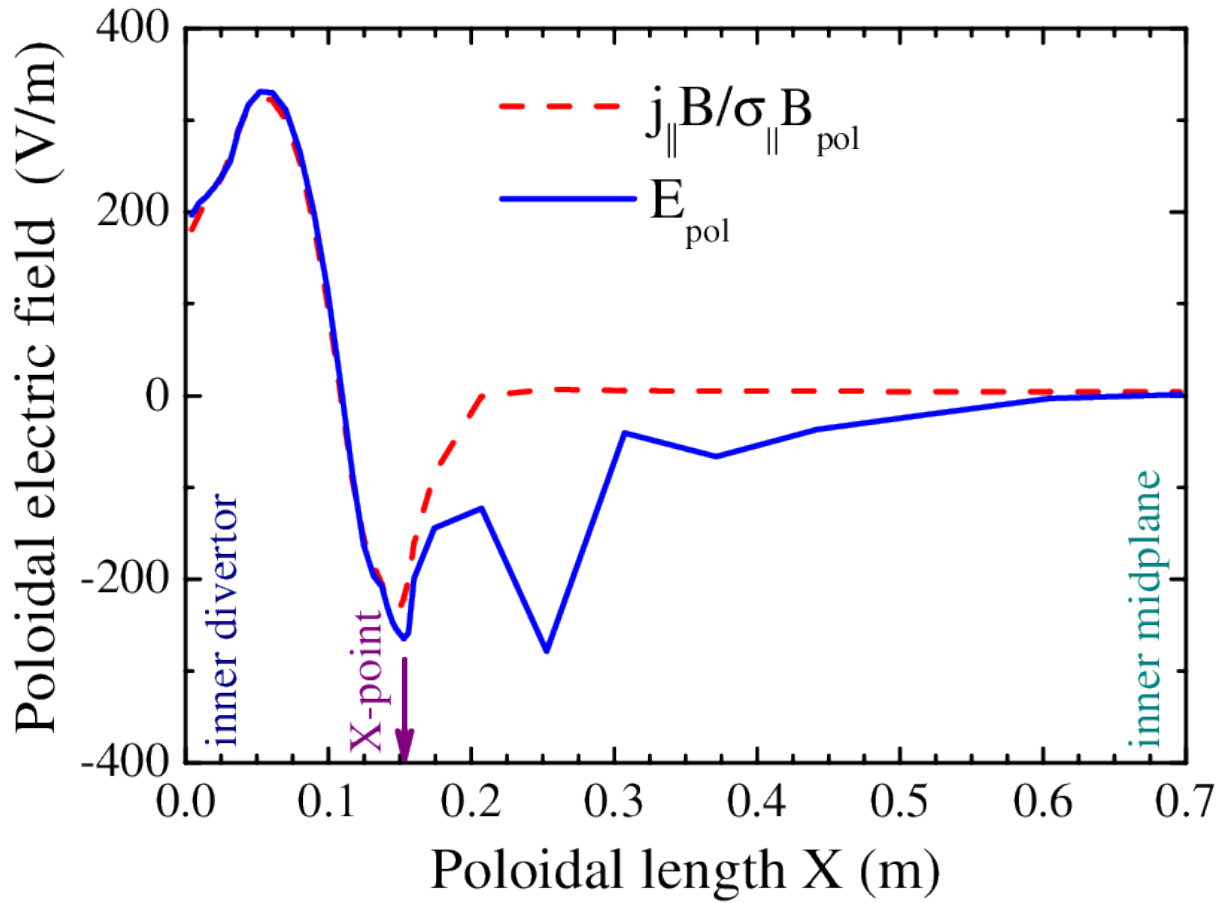


Figure 2. Poloidal electric field $E_{pol} = BE_{\parallel} / B_{pol}$ and corresponding parallel current (l.h.s of Eq. (2)), plotted versus poloidal length measured from inner target to the inner equatorial midplane. B_{pol} – poloidal magnetic field, B – absolute value of full magnetic field.

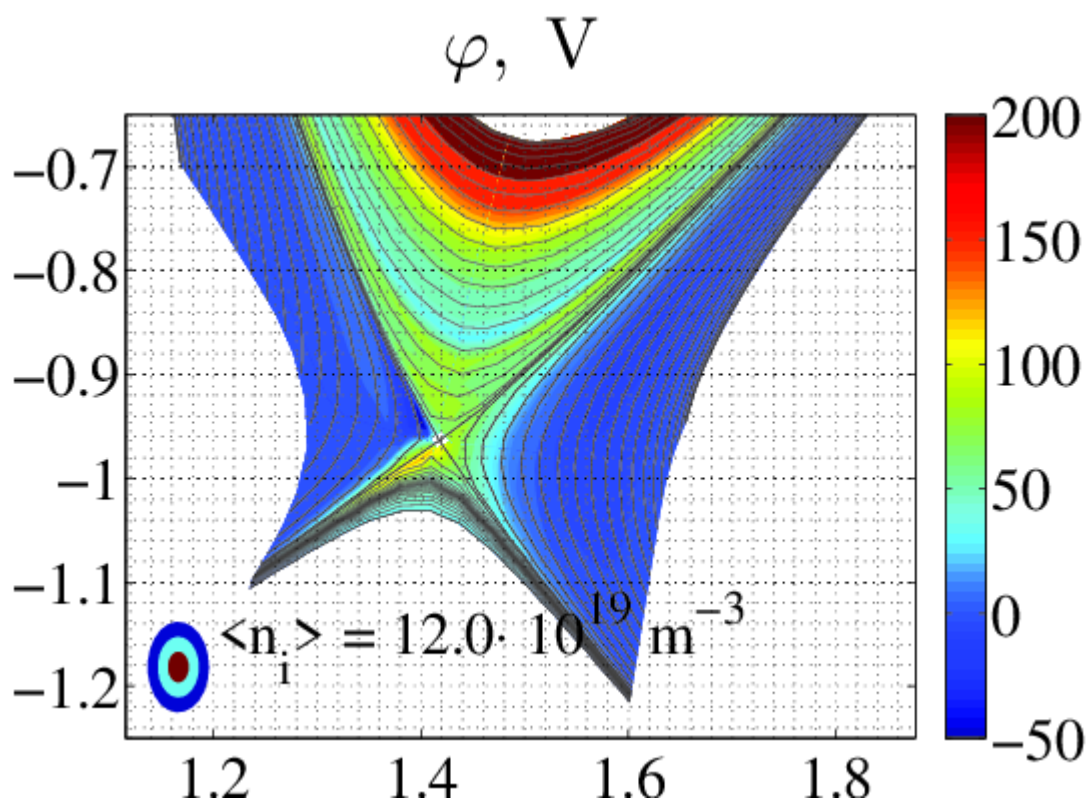
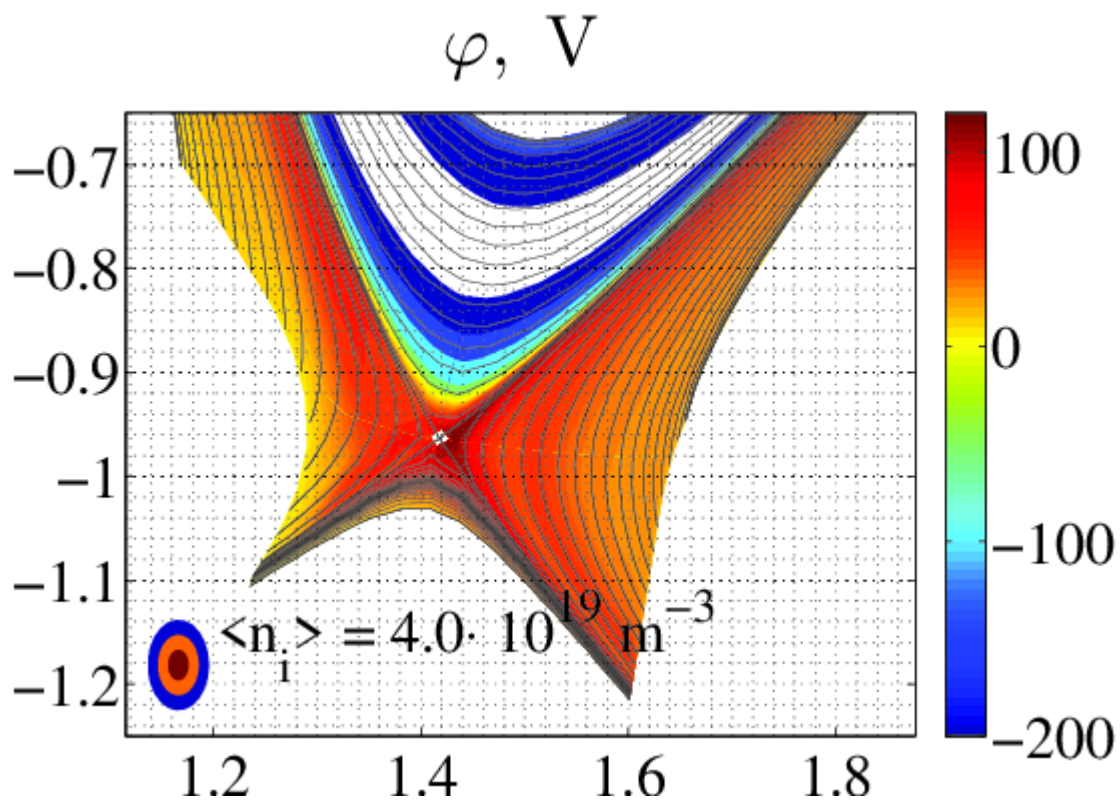


Figure 3. Calculated electric potential for different plasma density a) $\langle n_i \rangle = 4.0 \cdot 10^{19} \text{ m}^{-3}$ and b) $\langle n_i \rangle = 12.0 \cdot 10^{19} \text{ m}^{-3}$.